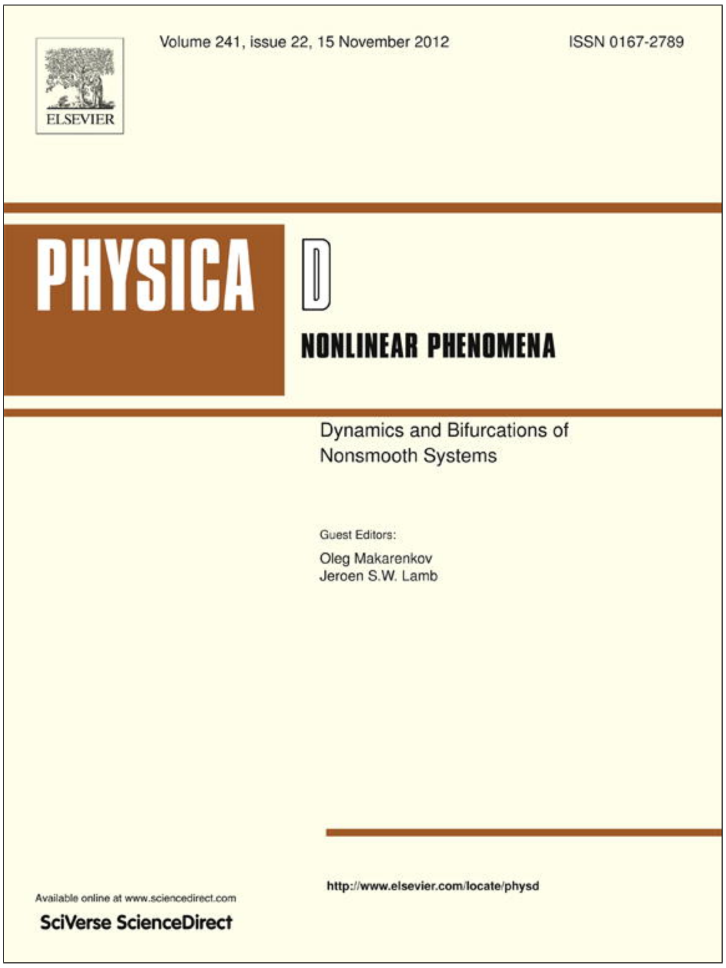
Volume 241, issue 22, 15 November 2012
ISSN 0167-2789
ELSEVIER
PHYSICA D
NONLINEAR PHENOMENA
Dynamics and Bifurcations of Nonsmooth Systems
Guest Editors:
Oleg Makarenkov
Jeroen S.W. Lamb
http://www.elsevier.com/locate/physd
Available online at www.sciencedirect.com
SciVerse ScienceDirect

Physica D 241 (2012) 2029–2041

Contents lists available at SciVerse ScienceDirect

Physica D

journal homepage: www.elsevier.com/locate/physd

Global uniform symptotic attractive stability of the non-autonomous bouncing ball system

R.I. Leine *, T.F. Heimsch

Institute of Mechanical Systems, Department of Mechanical and Process Engineering, ETH Zurich, CH-8092 Zurich, Switzerland

ARTICLE INFO

Article history:
Available online 5 May 2011

Keywords:
Stability theory
Finite-time attractivity
Impact
Measure differential inclusions

ABSTRACT

The non-autonomous bouncing ball system consists of a point mass in a constant gravitational field, which bounces inelastically on a flat vibrating table. A sufficient condition for the global uniform attractive stability of the equilibrium of the non-autonomous bouncing ball system is proved in this paper by using a Lyapunov-like method which can be regarded as an extension of Lyapunov's direct method to Lyapunov functions which may also temporarily increase along solution curves. The presented Lyapunov-like method is set up for non-autonomous measure differential inclusions and constructs a decreasing step function above the oscillating Lyapunov function. Furthermore, it is proved that the attractivity of the equilibrium of the bouncing ball system is symptotic, i.e. there exists a finite time for which the solution has converged exactly to the equilibrium. For this attraction time, an upper-bound is given in this paper.

1. Introduction

In this paper, the stability properties of the bouncing ball system on a vibrating table are studied in detail using and extending Lyapunov techniques for non-smooth systems. The main result of the paper is a novel Lyapunov-like method for the stability analysis of a class of non-autonomous measure differential inclusions. The proposed Lyapunov technique for non-smooth dynamical systems, which we present in the form of a theorem, can be regarded as an extension of Lyapunov's direct method to Lyapunov functions which may also temporarily increase along solution curves. The merit of the proposed Lyapunov-like method is that it allows to choose more natural Lyapunov candidate functions, e.g. energy-like functions or other functions with a clear physical meaning.

The stability of non-smooth dynamical systems is a novel research field which is receiving much attention in the mathematical as well as engineering community. Mechanical systems with impact phenomena and unilateral constraints form an important class of non-smooth systems as they arise in many engineering applications [1].

Non-smooth dynamical systems, with or without impulsive dynamics, are studied by various scientific communities using different mathematical frameworks [2] such as singular perturbations, switched or hybrid systems, complementarity systems, and (measure) differential inclusions.

The singular perturbation approach replaces the non-smooth system by a singularly perturbed smooth system. The resulting ordinary differential equation is extremely stiff and hardly suited for numerical integration as the artificial compliances induce spurious oscillations in the system. The singular perturbation technique for representing non-smooth dynamics can be useful for analytical studies, e.g. the limiting case where the 'stiffness' of the constraint becomes infinitely large [3]. However, possible stationary states, which exist in the non-smooth dynamical system, may be lost due to smoothening. For instance, the stationary state of a block on a rough slope cannot be described by a smoothed friction model for which the friction force vanishes at zero relative velocity (as the block will always slide). Therefore, this framework can generally not be used to study stability properties of non-smooth systems.

In the field of systems and control theory, the term hybrid system is frequently used for systems composed of continuous differential equations and discrete event parts [4–8]. The switched or hybrid system concept switches between differential equations with possible state re-initializations at the switching time-instants [8–11]. Of special interest are accumulation points which are called Zeno points in the hybrid systems literature, i.e. infinitely many switching events which occur in a finite time such as a bouncing ball coming to rest on a table. The hybrid systems approach deals with accumulation points by letting the solution before the accumulation point fulfil the differential equation and reset map, and extending the solution after the accumulation point with an additional part (e.g. for the classical bouncing ball system this is the zero solution). A problem with the hybrid systems concept is that the state of persistent contact, i.e. the ball being at rest on the table, is not described by the differential equation

* Corresponding author. Tel.: +41 16327792.
E-mail addresses: remco.leine@imes.mavt.ethz.ch (R.I. Leine), heimsch@imes.mavt.ethz.ch (T.F. Heimsch).

0167-2789/$ – see front matter © 2011 Elsevier B.V. All rights reserved.
doi:10.1016/j.physd.2011.04.013

(see for instance the hybrid system description of the bouncing ball in [5]). For this reason, the total solution is pieced together by the hybrid systems concept, where the post-Zeno part does not fulfil the differential equation. From this perspective, the hybrid systems concept does not describe the complete solution through an integration process on a differential equation (or a generalization of that). Moreover, a numerical technique based on the hybrid systems concept can only consider a finite number of switching points and will therefore not be able to proceed over the accumulation point.

Systems described by differential equations with a discontinuous right-hand side, but with a time-continuous state, can be extended to differential inclusions with a set-valued right-hand side [12]. The differential inclusion concept gives a simultaneous description of the dynamics in terms of a single inclusion, which avoids the need to switch between different differential equations. Moreover, this framework is able to describe accumulation points of switching events through an integration process. Systems which expose discontinuities in the state and/or vector field can be described by measure differential inclusions [4,13–15]. The differential measure of the state vector does not only consist of a part with a density with respect to the Lebesgue measure (i.e. the time derivative of the state vector), but is also allowed to contain an atomic part. The dynamics of the system is described by an inclusion of the differential measure of the state to a state-dependent set (similar to the concept of differential inclusions). Consequently, the measure differential inclusion concept describes the continuous dynamics as well as the impulsive dynamics with a single statement in terms of an inclusion and is able to describe accumulation phenomena with impact through an integration process. Moreover, the framework of measure differential inclusions leads directly to a numerical discretization, called the time-stepping method [14], which is a robust algorithm to simulate the dynamics of non-smooth systems. The framework of measure differential inclusions allows us to describe systems with state discontinuities and this framework is therefore more general than differential inclusions. However, the great advantage of this framework over other frameworks is, that physical interaction laws, such as friction and impact in mechanics or diode characteristics in electronics, can be formulated as set-valued force laws and be seamlessly incorporated in the formulation [1,16].

Stability properties of non-smooth systems are essential both in bifurcation analysis and the control of such systems. The analysis of bifurcation phenomena in non-smooth systems has received much attention lately in literature and conferences (see [2,17,18,11] and references therein). Many novel bifurcation phenomena have been revealed, but the progress of the analysis of bifurcations is hampered by a lack of tools to prove the presence and loss of stability in non-smooth systems. Currently, many research efforts are employed to develop stabilizing controllers for non-smooth systems, aiming at the stabilization of equilibria (i.e. solving the stabilization problem), see e.g. [19–25] and many others. In this context, previous work of the authors [26–30,15] focused on the stability properties of equilibrium sets for non-smooth dynamical systems. Moreover, in [19] stability properties of an equilibrium of measure differential inclusions of Lur'e-type are studied. The Lagrange–Dirichlet stability theorem is extended in [19] to measure differential inclusions describing mechanical systems with frictionless impact. However, many control problems, such as tracking control, output regulation, synchronization and observer design require the stability analysis of time-varying solutions, or, equivalently, of stationary solutions of time-varying systems. The research on the stability properties of time-varying non-smooth (mechanical) systems is still in its infancy and the current paper should be placed in this context.

In order to study Lyapunov stability criteria of equilibria in non-smooth non-autonomous (i.e. explicitly time-dependent) mechanical systems with unilateral constraints, we investigate the stability of the equilibrium of an apparently simple mechanical system meeting the requirements of non-smoothness and explicit time dependence. A standard problem of chaotic dynamics, which has been extensively studied in the literature, is a ball in a constant gravitational field bouncing inelastically on a flat vibrating table. The governing equations of motion are highly nonlinear due to the unilateral contact and generally do not allow for any closed form solution. The vast amount of papers on the bouncing ball system rather deals with the approximate description of chaos, periodic attractors or control of the bouncing ball system, e.g. to fix a periodic orbit at a defined height [31–36]. Up to now, very little attention has been paid to the stability properties of the equilibrium, i.e. the stationary motion of the ball for which it is at rest on the vibrating table.

In a brief communication of the authors [37], a sufficient condition for global symptotic (i.e. finite time) attractive stability of the equilibrium of the bouncing ball system with a harmonically vibrating table is proved by using a Lyapunov-like method with a simple energy-like Lyapunov function. The Lyapunov function is not always decreasing but a decreasing step function above the oscillating Lyapunov function is found. The equilibrium is proved to be globally symptotically attractively stable if it holds that

$$\frac{A\Omega^2}{g} < \frac{1-\varepsilon^2}{1+\varepsilon^2}, \tag{1}$$

where A and Ω are the amplitude and frequency of the harmonically vibrating table and ε is the restitution coefficient. Furthermore, an upper-bound for the attraction time is given in [37].

In a recent paper of Or and Teel [38] the bouncing ball system with an arbitrary motion of the table and constant restitution coefficient is studied. A very sophisticated Lyapunov function is presented in [38] with which a condition for the global uniform symptotic attractive stability of the equilibrium is derived by using Lyapunov's direct method. The condition can be put in the form

$$\varepsilon^2 \frac{g + a_{\max}}{g + a_{\min}} < 1, \tag{2}$$

where $a_{\max}$ and $a_{\min}$ are the maximal and minimal acceleration of the table, respectively.[1] For a harmonically vibrating table, with $a_{\max} = -a_{\min} = A\Omega^2$, one can easily show the equivalence of (1) and (2). The merit of the work of [38] is that it provides a wonderful Lyapunov function for the stability analysis of the bouncing ball system using a standard Lyapunov argument (a strictly decreasing Lyapunov function). However, the sophistication of the Lyapunov function makes it also very specific which limits the use if the system is slightly altered and a (totally) new Lyapunov function has to be found. For instance, if the restitution coefficient is made time-dependent with a known upper-bound, then the Lyapunov (candidate) function of [38] is no longer decreasing and the adaptation of the Lyapunov function is far from evident. The specific use of Lyapunov functions and their lack of physical meaning is of course a general problem with the direct method of Lyapunov.

In this paper, the Lyapunov-like method, which has been used by the authors in [37] to study the bouncing ball system with harmonic excitation, is generalized to the stability analysis of a class of measure differential inclusions. A Lyapunov technique to prove the conditional global uniform attractive stability of the equilibrium is presented in this paper. The Lyapunov technique

[1] The quantities $a_{\max}$ and $a_{\min}$ have a slightly different meaning in [38].

can be regarded as an extension of Lyapunov's direct method to Lyapunov functions which may also temporarily increase along solution curves. The presented Lyapunov-like method is set up for non-autonomous measure differential inclusions and constructs a decreasing step function above the oscillating Lyapunov function.

A sufficient condition for the global uniform symptotic attractive stability of the equilibrium of the bouncing ball system with an arbitrary motion of the table and a time-varying restitution coefficient is proved by using the presented Lyapunov-like method. The results of [37] are therefore proved in a much more rigorous way. Furthermore, it is proved that the attractivity of the equilibrium of the bouncing ball system is symptotic, i.e. there exists a finite time for which the solution has converged exactly to the equilibrium. For this attraction time, an upper-bound is given in this paper.

The paper is organized as follows. The equations of motion, the impact equation and the contact laws of the bouncing ball system are presented in Section 2. Section 3 makes the reader familiar with measure differential inclusions (MDIs) and puts the bouncing ball system in this framework. Stability properties of MDIs are defined in Section 4 and a theorem for the global uniform attractive stability is presented. Subsequently, this theorem is used in Section 5 to prove a sufficient condition for global uniform attractive stability of the bouncing ball system and an upper-bound for the attraction time is derived. Periodic motion is briefly considered in Section 6 showing the conservativeness of the stability results. Finally, conclusions are given in Section 7.

2. The bouncing ball system

The bouncing ball system consists of a rigid ball with mass m bouncing in a constant gravitational field g on a flat table which is moving vertically (see Fig. 1(a)). The bouncing ball system is equivalent to the forced system depicted in Fig. 1(b): a ball with a forcing $m\ddot{e}(t)$ bouncing on a fixed table. In the following, we will concentrate on the bouncing ball system, but it is sometimes important to realize the equivalence with the forced system. We will consider the movement $e(t) \in \mathcal{C}^\infty$ of the table to be a kinematic excitation, i.e. the mass of the table is considered to be much larger than the mass of the ball such that the movement $e(t)$ is not influenced by the motion of the ball. To keep the system as simple as possible only vertical motion is considered, leading to a system with one degree of freedom. The vertical position of the ball is addressed by the absolute coordinate $q(t)$. The velocity $u(t)$ of the ball agrees for almost all time-instants with $\dot{q}(t)$, except for time-instants t_n for which an impact between the ball and the table occurs. The velocity jumps instantaneously at collision time-instants t_n from the pre-impact velocity $u^-(t_n)$ to the post-impact velocity $u^+(t_n)$. The contact distance g_N between the ball and table, given by

$$g_N(t) = q(t) - e(t) \geq 0, \tag{3}$$

is non-negative because of impenetrability of the rigid ball and the table. The relative contact velocity

$$\gamma_N(t) = u(t) - \dot{e}(t) \tag{4}$$

agrees with $\dot{g}_N(t)$ whenever the velocity $u(t)$ exists. Similarly, we speak of the relative pre- and post-impact velocity

$$\gamma_N^\pm(t) = u^\pm(t) - \dot{e}(t) \tag{5}$$

at collision time-instants $t = t_n$.

The non-impulsive dynamics of the ball is described by the equation of motion

$$m\dot{u}(t) = -mg + \lambda_N(t), \tag{6}$$

where $\lambda_N(t)$ is the contact force between the ball and the table and mg is the weight of the ball. The contact force can be positive when

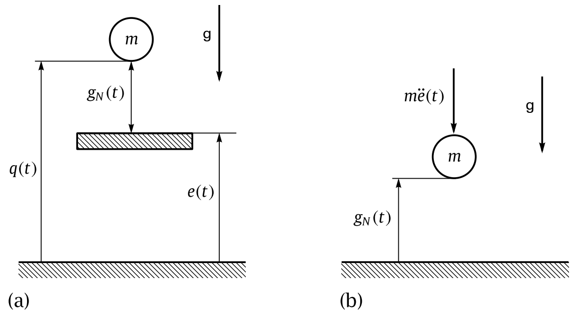

Fig. 1. The bouncing ball system (a) and the equivalent forced system (b).

contact is present ($g_N = 0$), but must vanish when the contact is open ($g_N > 0$). The contact force λ_N is non-negative because the ball and table can only push on each other in the absence of adhesion. The constitutive behaviour of the unilateral contact force λ_N is therefore described by Signorini's law

$$g_N(t) \geq 0, \qquad \lambda_N(t) \geq 0, \qquad g_N(t)\lambda_N(t) = 0, \tag{7}$$

which is an inequality complementarity condition between the dual variables g_N and λ_N.

The impulsive dynamics is described by the impact equation

$$m\left(u^+(t) - u^-(t)\right) = \Lambda_N(t), \tag{8}$$

where $\Lambda_N(t)$ is the contact impulse which causes an instantaneous velocity jump. Naturally, the contact impulse vanishes if the contact is open:

$$g_N(t) > 0: \quad \Lambda_N(t) = 0. \tag{9}$$

For time-instants for which the contact is closed ($g_N(t) = 0$) we will consider a Newton-type of restitution law expressed by the inequality complementarity condition

$$g_N(t) = 0: \quad \xi_N(t) \geq 0, \quad \Lambda_N(t) \geq 0, \quad \xi_N(t)\Lambda_N(t) = 0, \tag{10}$$

where $\xi_N(t) = \gamma_N^+(t) + \varepsilon(t)\gamma_N^-(t)$ and $\varepsilon(t)$ is Newton's coefficient of restitution. We consider the restitution coefficient $\varepsilon(t) \in \mathcal{C}^0$ to be time-dependent with the restriction

$$0 \leq \varepsilon(t) \leq \bar{\varepsilon} < 1 \quad \forall t. \tag{11}$$

The inequality complementarity condition (10) implies that a positive contact impulse $\Lambda_N(t) > 0$ can only be transmitted by the contact if $\xi_N(t) = 0$, i.e. if Newton's restitution law

$$\gamma_N^+(t) = -\varepsilon(t)\gamma_N^-(t) \tag{12}$$

holds. Similarly, if $\xi_N(t) > 0$, then the contact impulse $\Lambda_N(t)$ must vanish. Using the impact Eq. (8) together with $\Lambda_N(t) = 0$, we infer that there is no velocity jump ($u^+(t) = u^-(t)$). The relative velocity $\gamma_N(t)$ therefore also remains continuous and $\xi_N(t) > 0$ therefore implies that the momentarily closed contact will open ($\gamma_N(t) > 0$).

In the following, the kinematic excitation $e(t)$ of the table will be assumed to be analytic and to satisfy the bounds

$$a_{\min} \leq \ddot{e}(t) \leq a_{\max} \quad \forall t. \tag{13}$$

The velocity and the acceleration of the table are given by the continuous functions $\dot{e}(t)$ and $\ddot{e}(t)$, respectively.

We say that the ball is in persistent contact with the table at time t_0 if $g_N(t) = 0$ on some time interval $[t_0, t^*]$. While being in persistent contact, it therefore holds that $\gamma_N(t) = \dot{\gamma}_N(t) = 0$ for $t \in (t_0, t^*)$ from which we retrieve the contact force $\lambda_N(t)$ during persistent contact:

$$\lambda_N(t) = m\ddot{e}(t) + mg. \tag{14}$$

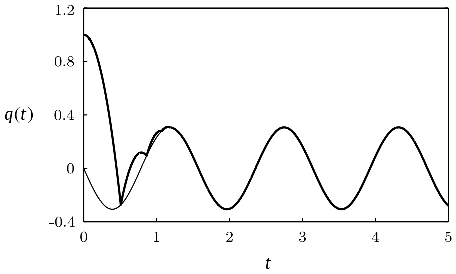

(a) $\kappa = 0.5 < \bar{\kappa}$.

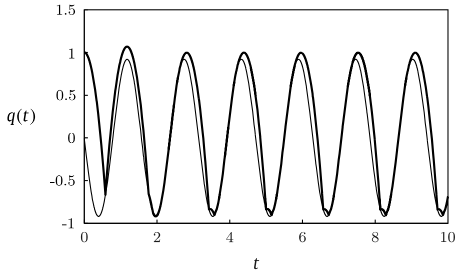

(b) $\kappa = 1.5 > \bar{\kappa}$.

Fig. 2. Trajectories of the bouncing ball system for $\varepsilon = 0.4$ with the same initial condition ($g_N(0) = 1$, $\gamma_N(0) = 0$) and different relative acceleration κ.

Detachment occurs at $t = t^*$ if the condition $\dot{\gamma}_N(t) = 0$ can no longer be fulfilled, that is if $m\ddot{e}(t) + m\mathrm{g} < 0$. We conclude that if the condition

$$\text{equilibrium condition:} \quad a_{\min} + \mathrm{g} \geq 0 \tag{15}$$

holds, then a ball which is initially on the table will remain on the table for all future times. We will refer to this steady state behaviour as the equilibrium position of the ball.

Throughout the paper, illustrations are given based on the assumption that the kinematic excitation $e(t) = -A\sin(\Omega t)$ is harmonic with the amplitude A and the angular frequency Ω, and we will use the ratio of the maximum acceleration $A\Omega^2$ of the table and the gravitational acceleration g

$$\kappa := \frac{A\Omega^2}{\mathrm{g}}, \tag{16}$$

which we call the relative acceleration of the table. For harmonic excitation it holds that

$$a_{\min} = -A\Omega^2, \qquad a_{\max} = A\Omega^2. \tag{17}$$

Furthermore, the equilibrium condition (15) in the case of harmonic excitation reads as $\mathrm{g} - A\Omega^2 \geq 0$ and can be expressed using the relative acceleration (16) as

$$\text{equilibrium condition:} \quad \kappa \leq 1 =: \bar{\kappa}. \tag{18}$$

Fig. 2(a) and (b) show trajectories of the bouncing ball system for harmonic excitation and clearly illustrate the significance of the equilibrium condition $\kappa \leq 1$. The position $q(t)$ of the ball quickly converges to the position $e(t)$ of the table in Fig. 2(a), i.e. the solution is attracted to the equilibrium. The trajectory $q(t)$ in Fig. 2(b) also converges to $e(t)$, but the contact is eventually lost because $\kappa > 1$, and the motion becomes periodic with intermittent phases of contact.

3. Measure differential inclusions

In this section we express the dynamics of the bouncing ball system in the form of a measure differential inclusion which allows us to describe the impulsive and non-impulsive dynamics in a unified way. The framework of measure differential inclusions originates in the work of Moreau [14,39,13] and forms together with the concept of set-valued force laws (see [1]) the mathematical foundation of modern non-smooth mechanics. For a detailed description of the measure differential inclusion framework for mechanical systems, the reader is referred to [40,4,15].

Let $\boldsymbol{x}(t)$ be the state of the dynamical system, being a function of locally bounded variation in time, of which the evolution is described by the measure differential inclusion

$$\mathrm{d}\boldsymbol{x}(t) \in \mathrm{d}\boldsymbol{\Gamma}(t, \boldsymbol{x}(t)). \tag{19}$$

The state $\boldsymbol{x}(t)$ has to be interpreted as the result of an integration process over the differential measure $\mathrm{d}\boldsymbol{x}$,

$$\boldsymbol{x}^+(t) = \boldsymbol{x}^-(t_0) + \int_{[t_0,t]} \mathrm{d}\boldsymbol{x}, \quad t \geq t_0, \tag{20}$$

where the integration process takes the left limit $\boldsymbol{x}^-(t_0)$ of the initial value to the right limit $\boldsymbol{x}^+(t)$ of the final value over the compact time interval $[t_0, t]$. A function of locally bounded variation can be decomposed in an absolutely continuous function $\boldsymbol{x}_{\mathrm{abs}}(t)$, a step function $\boldsymbol{x}_s(t)$ and a singular (Cantor-like) function. In mechanics there is no need to consider the singular part and we will tacitly assume that the state $\boldsymbol{x}(t)$ is a function of 'special' bounded variation, i.e. the singular part is assumed to vanish. The differential measure $\mathrm{d}\boldsymbol{x}$ therefore contains a density $\dot{\boldsymbol{x}}(t)$ with respect to the differential Lebesgue measure $\mathrm{d}t$ and contains a density $\boldsymbol{x}^+ - \boldsymbol{x}^-$ with respect to the differential atomic measure $\mathrm{d}\eta$,

$$\mathrm{d}\boldsymbol{x} = \dot{\boldsymbol{x}}\,\mathrm{d}t + (\boldsymbol{x}^+ - \boldsymbol{x}^-)\mathrm{d}\eta. \tag{21}$$

The Lebesgue part $\dot{\boldsymbol{x}}\,\mathrm{d}t$ in Eq. (21) is the differential measure of the absolutely continuous function $\boldsymbol{x}_{\mathrm{abs}}(t)$ and describes the continuous variation of $\boldsymbol{x}(t)$. The atomic part $(\boldsymbol{x}^+ - \boldsymbol{x}^-)\mathrm{d}\eta$ is the differential measure of the step function $\boldsymbol{x}_s(t)$ and is used to describe discontinuities in $\boldsymbol{x}(t)$. The upper and lower limits of $\boldsymbol{x}(t)$ at impulsive time-instants t_n are denoted by $\boldsymbol{x}^+(t_n) := \lim_{t\downarrow t_n} \boldsymbol{x}(t)$ and $\boldsymbol{x}^-(t_n) := \lim_{t\uparrow t_n} \boldsymbol{x}(t)$, respectively. Note that $\int_I (\cdot)\mathrm{d}\eta = 0$ if the function $\boldsymbol{x}(t)$ is absolutely continuous on I. If $\mathrm{d}\boldsymbol{x}$ is integrated over a singleton $\{t_n\}$, then $\int_{\{t_n\}} (\cdot)\mathrm{d}t = 0$ and $\int_{\{t_n\}} \mathrm{d}\boldsymbol{x} = \boldsymbol{x}^+(t_n) - \boldsymbol{x}^-(t_n)$, where the latter reduces to zero if the function $\boldsymbol{x}$ is continuous at t_n. In the following, we will use the notation $\boldsymbol{\varphi}(t, t_0, \boldsymbol{x}_0)$ for a solution curve $\boldsymbol{x}(t)$ with the initial condition $\boldsymbol{x}^-(t_0) = \boldsymbol{x}_0$. The solution starting from a specific initial condition $(t_0, \boldsymbol{x}_0)$ is generally not unique in forward time.

We describe the motion of the bouncing ball system with the state vector $\boldsymbol{x}(t)$ chosen as

$$\boldsymbol{x}(t) := \begin{bmatrix} x_1(t) \\ x_2(t) \end{bmatrix} = \begin{bmatrix} g_N(t) \\ \gamma_N(t) \end{bmatrix}, \tag{22}$$

such that the equilibrium position is located at the origin $\boldsymbol{x}^* = \boldsymbol{0}$. The gap function $x_1(t) = g_N(t)$ is an absolutely continuous function in time and its differential measure only consists of a Lebesgue part:

$$\mathrm{d}x_1(t) = x_2(t)\mathrm{d}t. \tag{23}$$

The relative velocity $x_2(t) = \gamma_N(t)$ is considered to be a function of special locally bounded variation which is discontinuous at collision time-instants t_n. The non-impulsive dynamics of the ball is described by the equation of motion (6), now written in terms of $x_2(t) = \gamma_N(t)$ as

$$\dot{\gamma}_N(t) = -(\mathrm{g} + \ddot{e}(t)) + \frac{1}{m}\lambda_N(t), \tag{24}$$

and the impulsive dynamics is governed by the impact equation (8)

$$\gamma_N^+(t) - \gamma_N^-(t) = \frac{1}{m}\Lambda_N(t). \tag{25}$$

The equation of motion (24) and the impact equation (25) can be combined in a single equality of measures

$$\mathrm{d}\gamma_N(t) = -\left(\mathrm{g} + \ddot{e}(t)\right) + \frac{1}{m}\mathrm{d}P_N(t), \tag{26}$$

where the differential measure

$$\mathrm{d}P_N(t) = \lambda_N(t)\mathrm{d}t + \Lambda_N(t)\mathrm{d}\eta \tag{27}$$

contains the total contact percussion of the forces/impulses that act on the ball. The constitutive behaviour of the contact force λ_N is described by Signorini's law (7), which is a set-valued force law on position level, whereas the constitutive behaviour of the contact impulse Λ_N is described by the impact law (10), being a set-valued force law on velocity level. We now gather these constitutive descriptions into one set-valued force law for $\mathrm{d}P_N$ on velocity level. If we impose Signorini's law (7) at all time-instants and consider a time-instant t for which the ball is in persistent contact ($g_N(t) = 0$), then it follows that

$$\gamma_N(t) \geq 0, \qquad \lambda_N(t) \geq 0, \qquad \gamma_N(t)\lambda_N(t) = 0, \tag{28}$$

which is an inequality complementary condition on velocity level. For a non-impulsive time-instant it holds that $\xi_N(t) = \gamma_N^+(t) + \varepsilon(t)\gamma_N^-(t) = (1 + \varepsilon(t))\,\gamma_N(t)$ and (28) is equivalent to

$$\xi_N(t) \geq 0, \qquad \lambda_N(t) \geq 0, \qquad \xi_N(t)\lambda_N(t) = 0, \tag{29}$$

which is of the same form as the impact law (10). The constitutive behaviour of the total contact percussion for a closed contact ($g_N(t) = 0$) can therefore be expressed as

$$\xi_N(t) \geq 0, \qquad \mathrm{d}P_N(t) \geq 0, \qquad \xi_N(t)\mathrm{d}P_N(t) = 0, \tag{30}$$

noting that $\mathrm{d}t$ and $\mathrm{d}\eta$ are non-negative measures. More conveniently, the inequality complementarity (30) can be cast in a normal cone inclusion (see [15])

$$-\mathrm{d}P_N \in N_{T_{\mathcal{K}}(g_N)}(\xi_N) = \begin{cases} \mathbb{R}_0^- & g_N = \xi_N = 0, \\ 0 & \text{else}, \end{cases} \tag{31}$$

where $T_{\mathcal{K}}(g_N)$ is the tangent cone on the set $\mathcal{K} = \{g_N \in \mathbb{R} \mid g_N \geq 0\}$ of admissible positions.

The dynamics of the bouncing ball system can therefore be given in terms of a non-autonomous measure differential inclusion

$$\mathrm{d}\boldsymbol{x} \in \begin{bmatrix} x_2\mathrm{d}t \\ -\left(\mathrm{g} + \ddot{e}(t)\right)\mathrm{d}t + \dfrac{1}{m}N_{T_{\mathcal{K}}(g_N)}(\xi_N) \end{bmatrix} =: \mathrm{d}\boldsymbol{\Gamma}(t, \boldsymbol{x}), \tag{32}$$

where $\xi_N(t) = x_2^+(t) + \varepsilon(t)x_2^-(t)$. The system (32) has the admissible set

$$\mathcal{A} = \{\boldsymbol{x} \in \mathbb{R}^2 \mid x_1 \in \mathcal{K}\} = \{\boldsymbol{x} \in \mathbb{R}^2 \mid x_1 \geq 0\}. \tag{33}$$

Due to the choice of the state $\boldsymbol{x}(t)$ in (22), both the sets $\mathcal{A}$ and $\mathcal{K}$ are time independent. The non-autonomicity of the system (32) is caused by explicit time dependence of the table acceleration $\ddot{e}(t)$. In this respect, also note the equivalence with the forced system depicted in Fig. 1(b).

In [41] it has been proved that the solution of the bouncing ball system is unique in forward time if the external excitation $e(t)$ of the table is an analytic function. For this reason we assume that $e(t)$ is analytic. Note that the solutions of the bouncing ball system are generally not unique in backward time. The bouncing ball system (32) is consistent in the sense that an admissible initial condition $\boldsymbol{x}_0 \in \mathcal{A}$ leads to an admissible solution curve $\boldsymbol{\varphi}(t, t_0, \boldsymbol{x}_0) \in \mathcal{A}$ for all $t \geq t_0$. We therefore have existence and uniqueness of solutions in forward time.

4. Lyapunov stability properties of MDI's

In this section, we define stability properties of measure differential inclusions of the form (19). Subsequently, we present a Lyapunov-like technique to prove the global uniform attractive stability of an equilibrium, being the key result of the paper.

Let us first precisely define an equilibrium point.

Definition 1 (*Equilibrium Point*)**.** A point $\boldsymbol{x}^*$ is called an equilibrium point of (19) if there exists a solution curve $\boldsymbol{\varphi}(t, t_0, \boldsymbol{x}^*)$ such that

$$\boldsymbol{\varphi}(t, t_0, \boldsymbol{x}^*) = \boldsymbol{x}^*, \quad \forall\, t \geq t_0.$$

Clearly, it must holds that $\mathbf{0} \in \mathrm{d}\boldsymbol{\Gamma}(t, \boldsymbol{x}^*)\ \forall\, t \geq t_0$ if $\boldsymbol{x}^*$ is an equilibrium point of (19).

An equilibrium point of a dynamical system which is both stable and locally/globally attractive is called in the literature locally/globally 'asymptotically stable'. Solution curves of a 'smooth' dynamical system (i.e. ODE's with a Lipschitz constant) can never meet each other because of the uniqueness of solutions in forward and backward time. The attractivity in smooth systems is therefore always *asymptotic* in the sense that neighbouring solution curves approach but never reach the equilibrium point when $t \to \infty$. The attractivity of an equilibrium point of a non-smooth system is not necessarily asymptotic as it might be reached in a finite time. We therefore refrain from the terminology 'asymptotic stability' to denote an equilibrium point which is both attractive and stable. Instead, we will use the terminology *attractive stability* [15]. If the solution curves converge asymptotically to the equilibrium point, then we speak of *asymptotic attractivity*. If the solution curves converge to the equilibrium point in finite time, then we speak of *symptotic attractivity*.

Definition 2 (*Symptotic Attractivity*)**.** An equilibrium point $\boldsymbol{x}^*$ of (19) is called symptotically attractive if there exists a $\delta > 0$ such that for any bounded $\boldsymbol{x}_0 \in \mathcal{A}$ and t_0 with

$$\|\boldsymbol{x}_0 - \boldsymbol{x}^*\| < \delta$$

each solution curve $\boldsymbol{\varphi}(\cdot, t_0, \boldsymbol{x}_0)$ reaches $\boldsymbol{x}^*$ in a finite time, i.e.

$$\boldsymbol{\varphi}(T + t_0, t_0, \boldsymbol{x}_0) = \boldsymbol{x}^*,$$

with $T = T(\boldsymbol{x}_0) < \infty$ for bounded $\boldsymbol{x}_0 \in \mathcal{A}$.

Remark. In the hybrid systems literature, the terminology 'Zeno' point is often used to denote points in the state space which are reached in finite time after infinitely many discrete events. In non-smooth mechanics such a point is denoted as (right) accumulation point. We emphasize that accumulation points/'Zeno' points are not necessarily equilibria. An example of a non-equilibrium accumulation point/'Zeno' point, being part of a periodic solution, is given in Section 6, see Fig. 6(f).

We will define global uniform attractive stability by making use of comparison functions. We briefly recall the definitions of comparison functions as given in [42]. A continuous function $\alpha : [0, a) \to [0, \infty)$ is said to belong to class $\mathcal{K}$ if it is strictly increasing and $\alpha(0) = 0$. It is said to belong to class $\mathcal{K}_\infty$ if $a = \infty$ and $\alpha(r) \to \infty$ as $r \to \infty$. A continuous function $\beta : [0, a) \times [0, \infty) \to [0, \infty)$ is said to belong to class $\mathcal{KL}$ if, for each fixed s, the mapping $\beta(r, s)$ belongs to class $\mathcal{K}$ with respect to r and, for each fixed r, the mapping $\beta(r, s)$ is decreasing with respect to s and $\beta(r, s) \to 0$ as $s \to \infty$.

Definition 3 (*Global Uniform Attractive Stability*)**.** An equilibrium point $\boldsymbol{x}^*$ of (19) is called globally uniformly attractively stable if there exists a class $\mathcal{KL}$ function β such that each solution curve $\boldsymbol{\varphi}(\cdot, t_0, \boldsymbol{x}_0)$ for $\boldsymbol{x}_0 \in \mathcal{A}$ satisfies

$$\|\boldsymbol{\varphi}(t, t_0, \boldsymbol{x}_0) - \boldsymbol{x}^*\| \leq \beta(\|\boldsymbol{x}_0 - \boldsymbol{x}^*\|, t - t_0),$$

for almost all $t \geq t_0$.

Remark. Stability properties are usually defined in terms of a Lyapunov ε–δ argument. Equivalently, one can characterize these stability properties by using comparison functions, see Appendix C.6 in [42]. The proof in [42], that the characterization with comparison functions implies the definition, is given for ordinary differential equations, but the proof does not use a solution concept and is therefore immediately valid for measure differential inclusions. The proof that the definition also implies the characterization is much more technical. Instead, we allow ourselves to take the characterization with comparison functions as *definition*. This line of reasoning is also taken in [43].

Remark. Definition 3 is a stability property of an *equilibrium point*. In [44,45] stability properties are presented for 'Zeno' points (i.e. accumulation points) within the solution concept of hybrid systems. The 'Zeno' points in [44,45] are not necessarily equilibria.

We now present a Lyapunov-like technique to prove global uniform attractive stability in the sense of Definition 3. Let t_0 denote the initial time-instant and $\boldsymbol{x}^-(t_0) = \boldsymbol{x}_0$ the initial condition. Doing so, we allow for a possible impulsive event at the initial time-instant $t = t_0$. Let $\{t_n\}$ denote the sequence of time-instants $\{t_1, t_2, t_3, \ldots, t_\infty\}$ for which the solution curve $\boldsymbol{x}(t) := \boldsymbol{\varphi}(t, t_0, \boldsymbol{x}_0)$ is discontinuous for $t > t_0$. The solution $\boldsymbol{x}(t)$ has an accumulation point if t_∞ is finite.

Theorem 1. *Let $\boldsymbol{x}^* = \boldsymbol{0}$ be an equilibrium point of (19). If there exists a positive definite function $V : \mathbb{R}^n \to \mathbb{R}_0^+ \cup \{+\infty\}$, being bounded on the admissible set $\mathcal{A}$ of (19), such that the step function $W(t)$ along solution curves of the system, defined by*

$$W(t) = \begin{cases} \sup\limits_{t\in[t_0,t_1]} V(\boldsymbol{x}^-(t)) & t \in [t_0, t_1] \\ V\left(\boldsymbol{x}^-(t_{n-1})\right) & t \in (t_{n-1}, t_n], n > 1 \\ 0 & t > t_\infty, \end{cases} \tag{34}$$

has the following properties

- *$W(t_1) \le \sigma(V(\boldsymbol{x}_0))$ for some class $\mathcal{K}$ function σ,*
- *$W(t)$ is decreasing in time,*
- *$W(t)$ satisfies $V(\boldsymbol{x}(t)) \le W(t)$ on each interval $t \in (t_{n-1}, t_n)$, $n > 1$,*
- *$W(t)$ converges to zero for $t \to t_\infty$, i.e. $\lim_{t\to t_\infty} W(t) = 0$,*

then the equilibrium $\boldsymbol{x}^*$ is globally uniformly attractively stable.

Proof. If V is a positive definite function which is bounded on $\mathcal{A}$, then there exist functions α_1 and α_2 of class $\mathcal{K}_\infty$ such that

$$\alpha_1(\|\boldsymbol{x}\|) \le V(\boldsymbol{x}) \le \alpha_2(\|\boldsymbol{x}\|) \quad \forall \boldsymbol{x} \in \mathcal{A}. \tag{35}$$

The function $W(t)$ therefore satisfies the inequality

$$W(t_0) = W(t_1) \le \sigma(V(\boldsymbol{x}_0)) \le \sigma(\alpha_2(\|\boldsymbol{x}_0\|)). \tag{36}$$

Define the comparison function

$$\beta_W(W(t_1), t - t_0) = \begin{cases} W(t_1) & t_0 \le t \le t_1, \\ \dfrac{W(t_n) - W(t_{n-1})}{t_n - t_{n-1}}(t - t_{n-1}) + W(t_{n-1}) & t_{n-1} \le t \le t_n, \\ 0 & t \ge t_\infty, \end{cases} \tag{37}$$

where the second case holds for all $n > 1$. Clearly, β_W is a continuous function in both arguments. For fixed $t - t_0$, the mapping $\beta_W(W(t_1), t - t_0)$ is upper-bounded by $\beta_W(W(t_1), t - t_0) \le W(t_1)$, i.e. a class $\mathcal{K}$ function with respect to $W(t_1)$. For fixed $W(t_1)$, the mapping $\beta_W(W(t_1), t - t_0)$ is non-increasing with respect to $t - t_0$ and $\beta_W(W(t_1), t - t_0) \to 0$ as $t \to t_\infty$. Hence, β_W is upper-bounded by a class $\mathcal{KL}$ function $\overline{\beta}_W(W(t_1), t - t_0) = \beta_W(W(t_1), t - t_0) + W(t_1)e^{t_0 - t}$. It therefore holds that

$$\|\boldsymbol{x}(t)\| \le \alpha_1^{-1}\left(\overline{\beta}_W(\sigma(\alpha_2(\|\boldsymbol{x}_0\|)), t - t_0)\right) = \beta(\|\boldsymbol{x}_0\|, t - t_0), \tag{38}$$

for almost all $t \ge t_0$, where

$$\beta(x, t) = \alpha_1^{-1}\left(\overline{\beta}_W\left(\sigma\left(\alpha_2(x)\right)\right), t\right)$$

is a class $\mathcal{KL}$ function, which concludes the proof. □

5. The equilibrium of the bouncing ball system

In this section, we will use Theorem 1 to prove a sufficient condition for the global uniform attractive stability of the equilibrium of the bouncing ball system, see Proposition 1. Subsequently, we will prove that the attractivity is symptotic in Proposition 2.

Proposition 1 (*Global Uniform Attractive Stability*)**.** *Let the bouncing ball system (32) satisfy the bounds (13) on $e(t)$ and (11) on $\varepsilon(t)$ with $\mathrm{g} + a_{\min} > 0$. If it holds that*

$$\frac{\mathrm{g} + a_{\max}}{\mathrm{g} + a_{\min}}\bar{\varepsilon}^2 < 1, \tag{39}$$

then the equilibrium $\boldsymbol{x}^* = \boldsymbol{0}$ of the bouncing ball system is globally uniformly attractively stable.

Proof. Consider the Lyapunov candidate function

$$V(\boldsymbol{x}) = \frac{1}{2}x_2^2 + \tilde{\mathrm{g}}x_1 + \Psi_{\mathcal{K}}(x_1) = \frac{1}{2}\gamma_N^2 + \tilde{\mathrm{g}}g_N + \Psi_{\mathcal{K}}(g_N), \tag{40}$$

where $\Psi_{\mathcal{K}}(g_N)$ is the indicator function on the admissible set $\mathcal{K} = \mathbb{R}_0^+$ defined by

$$\Psi_{\mathcal{K}}(g_N) = \begin{cases} 0 & g_N \in \mathcal{K}, \\ \infty & \text{else}, \end{cases} \tag{41}$$

and $\tilde{\mathrm{g}} > 0$ is (for the moment) an arbitrary positive number. The function V is an energy-like Lyapunov function in terms of the relative coordinates g_N and γ_N. More specifically, if we take $\tilde{\mathrm{g}} = \mathrm{g}$, it is the total mechanical energy per unit mass of the equivalent forced system depicted in Fig. 1(b). The indicator function $\Psi_{\mathcal{K}}(g_N)$ plays the role of a potential for the contact force and is necessary to make V a positive definite function. The bouncing ball system is consistent in the sense that solutions remain in the admissible set $\mathcal{A}$ for admissible initial conditions. It therefore holds that $\Psi_{\mathcal{K}}(x_1(t)) = 0$ for all $t \ge t_0$ along solution curves of the system. With some abuse of notation we define $V(t) = V(\boldsymbol{x}(t))$ to be the Lyapunov candidate function evaluated along a solution curve $\boldsymbol{x}(t)$. Clearly, the function $V(t)$ is a function of special locally bounded variation because of its dependence on $x_2(t)$. The differential measure of $V(t)$ can therefore be decomposed into

$$\mathrm{d}V = \dot{V}\mathrm{d}t + \left(V^+ - V^-\right)\mathrm{d}\eta. \tag{42}$$

The function $V(t)$ is discontinuous at collision times t_n when the gap function $g_N(t_n)$ vanishes with $\gamma_N^-(t_n) < 0$. The jump height follows from the impact law (10)

$$\begin{aligned} V^+(t_n) - V^-(t_n) &= \frac{1}{2}\gamma_N^+(t_n)^2 - \frac{1}{2}\gamma_N^-(t_n)^2 \\ &= -\frac{1}{2}\left(1 - \varepsilon(t_n)^2\right)\gamma_N^-(t_n)^2 \end{aligned} \tag{43}$$

and, together with the bound (11), we obtain

$$V^+(t_n) - V^-(t_n) \le -\frac{1}{2}\left(1 - \bar{\varepsilon}^2\right)\gamma_N^-(t_n)^2 < 0, \tag{44}$$

from which we conclude that the Lyapunov candidate function V decreases over impacts. The time derivative of $V(t)$,

$$\dot{V} = \gamma_N \dot{\gamma}_N + \tilde{g}\gamma_N = -\gamma_N \ddot{e}(t) + \gamma_N (\tilde{g} - g), \tag{45}$$

depends explicitly on time and can be negative or positive such that the Lyapunov function may decrease or increase in between collisions. The acceleration $\ddot{e}(t)$ of the table satisfies the bounds $a_{\min} \le \ddot{e}(t) \le a_{\max}$, see (13). The maximal time derivative $\dot{V}$ is obtained if $\ddot{e}(t) = a_{\min}$ when $\gamma_N > 0$ and $\ddot{e}(t) = a_{\max}$ when $\gamma_N < 0$, which yields the conservative estimate

$$\dot{V} \le \begin{cases} (-a_{\min} + \tilde{g} - g)\,\gamma_N & \gamma_N \ge 0, \\ (-a_{\max} + \tilde{g} - g)\,\gamma_N & \gamma_N < 0, \end{cases} \tag{46}$$

and which we can write as

$$\dot{V} \le \frac{a_{\max} - a_{\min}}{2}|\gamma_N| + \left(-\frac{a_{\max} + a_{\min}}{2} + \tilde{g} - g\right)\gamma_N. \tag{47}$$

We now choose $\tilde{g}$ such that the last term in (47) vanishes, i.e.

$$\tilde{g} = g + \frac{a_{\max} + a_{\min}}{2}, \tag{48}$$

and we easily verify that this choice satisfies $\tilde{g} > 0$.

Define the step function $W(t)$ along solution curves $\boldsymbol{x}(t) = \boldsymbol{\varphi}(t, t_0, \boldsymbol{x}_0)$ of the system as in (34). The value of $W(t_1) = \sup_{t\in[t_0,t_1]} V(\boldsymbol{x}^-(t))$ is the maximum of $V(\boldsymbol{x}_0)$ and $\sup_{t\in(t_0,t_1)} V(t)$, where

$$V(t) = V^+(t_0) + \int_{t_0}^{t} \dot{V}(t)\,dt \le V^+(t_0) + \int_{t_0}^{t_1} |\dot{V}(t)|\,dt \tag{49}$$

on the open time interval (t_0, t_1). Using $V^+(t_0) \le V^-(t_0) = V(\boldsymbol{x}_0)$, together with (47)–(49), we can give an upper-bound for $W(t_1)$:

$$W(t_1) \le V(\boldsymbol{x}_0) + \frac{a_{\max} - a_{\min}}{2}\int_{t_0}^{t_1} |\gamma_N(t)|\,dt. \tag{50}$$

The integral $\int_{t_0}^{t_1} |\gamma_N(t)|dt$ is the total variation of the absolutely continuous function $g_N(t)$ on the time interval $[t_0, t_1]$. The gap function $g_N(t)$ is a concave function on each non-impulsive interval, because it holds that $\ddot{g}_N(t) = \dot{\gamma}_N(t) = -g - \ddot{e}(t) < 0$ due to the inequality

$$-g - a_{\max} \le \dot{\gamma}_N(t) \le -g - a_{\min} < 0. \tag{51}$$

The total variation of $g_N(t)$ on $[t_0, t_1]$ has therefore the upper-bound

$$\int_{t_0}^{t_1} |\gamma_N(t)|dt \le 2 \max_{[t_0,t_1]} g_N(t). \tag{52}$$

The gap function $g_N(t)$ is smooth on (t_0, t_1) and can be written as a Taylor series at t_0 with Lagrange form of the remainder term (Taylor's theorem as generalization of the mean value theorem):

$$g_N(t) = g_N(t_0) + \gamma_N^+(t_0)\,(t - t_0) + \frac{1}{2}\dot{\gamma}_N(\tilde{t})\,(t - t_0)^2 \tag{53}$$

for some $\tilde{t} \in (t_0, t)$. Using (51) we obtain the upper-bound

$$g_N(t) \le g_N(t_0) + \gamma_N^+(t_0)\,(t - t_0) - \frac{1}{2}(g + a_{\min})\,(t - t_0)^2. \tag{54}$$

The function $g_N(t)$ on $[t_0, t_1]$ is therefore bounded from above by

$$\begin{aligned} \max_{[t_0,t_1]} g_N(t) &\le g_N(t_0) + \frac{1}{2}\frac{\gamma_N^+(t_0)^2}{g + a_{\min}} \\ &\le \frac{1}{\tilde{g}}V(\boldsymbol{x}_0) + \frac{1}{g + a_{\min}}V(\boldsymbol{x}_0). \end{aligned} \tag{55}$$

Hence, using (50), (52) and (55), the value $W(t_1)$ is bounded from above by

$$W(t_1) \le \left(1 + \frac{a_{\max} - a_{\min}}{\tilde{g}} + \frac{a_{\max} - a_{\min}}{g + a_{\min}}\right)V(\boldsymbol{x}_0), \tag{56}$$

which is a class $\mathcal{K}_\infty$ function with respect to $V(\boldsymbol{x}_0)$.

The step function $W(t)$ is a left-continuous piecewise constant function with discontinuities at the collision time-instants $t = t_n$. The step height is

$$W(t_{n+1}) - W(t_n) = V^-(t_n) - V^-(t_{n-1}), \tag{57}$$

which can be interpreted as the cumulative change of V over one impact at the time-instant t_{n-1} and the subsequent non-impulsive interval (t_{n-1}, t_n), i.e.

$$\begin{aligned} W(t_{n+1}) - W(t_n) &= \int_{[t_{n-1},t_n)} dV \\ &= V^+(t_{n-1}) - V^-(t_{n-1}) + \int_{t_{n-1}}^{t_n} \dot{V}\,dt. \end{aligned} \tag{58}$$

Using (47) and (48), we can give an upper-bound for the last term in (58)

$$\int_{t_{n-1}}^{t_n} \dot{V}\,dt \le \frac{a_{\max} - a_{\min}}{2}\int_{t_{n-1}}^{t_n} |\gamma_N(t)|\,dt, \tag{59}$$

where $\int_{t_{n-1}}^{t_n} |\gamma_N(t)|dt$ is, again, the total variation of $g_N(t)$ on the time interval $[t_{n-1}, t_n]$. The steps in equations (51) to (55), which have been derived for the time interval $[t_0, t_1]$, are now repeated for the time interval $[t_{n-1}, t_n]$ using $g_N(t_{n-1}) = 0$:

$$\begin{aligned} \int_{t_{n-1}}^{t_n} |\gamma_N(t)|dt &= 2 \max_{[t_{n-1},t_n]} g_N(t) \\ &\le \frac{\gamma_N^+(t_{n-1})^2}{g + a_{\min}} \\ &\le \frac{\bar{\varepsilon}^2\gamma_N^-(t_{n-1})^2}{g + a_{\min}}. \end{aligned} \tag{60}$$

With the conservative estimates (44) and (60) the step height (58) of $W(t)$ is bounded from above by

$$\begin{aligned} &W(t_{n+1}) - W(t_n) \\ &\le \left(-\frac{1}{2}\left(1 - \bar{\varepsilon}^2\right) + \frac{a_{\max} - a_{\min}}{2}\frac{\bar{\varepsilon}^2}{g + a_{\min}}\right)\gamma_N^-(t_{n-1})^2. \end{aligned} \tag{61}$$

We now define

$$\alpha := \frac{g + a_{\max}}{g + a_{\min}}\bar{\varepsilon}^2. \tag{62}$$

Under condition (39) it holds that $0 \le \alpha < 1$ and therefore

$$-\frac{1}{2}\left(1 - \bar{\varepsilon}^2\right) + \frac{a_{\max} - a_{\min}}{2}\frac{\bar{\varepsilon}^2}{g + a_{\min}} = -\frac{1}{2}(1 - \alpha) < 0. \tag{63}$$

Substitution of $W(t_n) = V^-(t_{n-1}) = \frac{1}{2}\left(\gamma_N^-(t_{n-1})\right)^2$ in (61) gives an upper-bound for the discrete map $W(t_n) \mapsto W(t_{n+1})$

$$W(t_{n+1}) \le \alpha W(t_n), \tag{64}$$

which is a contraction map because $|\alpha| < 1$ and $W(t) \ge 0$ for all t. This implies that the function $W(t)$ is a decreasing step function converging to zero for $t \to t_\infty$.

Lastly, we prove that the step function $W(t)$ forms an upper-bound for the Lyapunov function $V(t)$. Without loss of generality

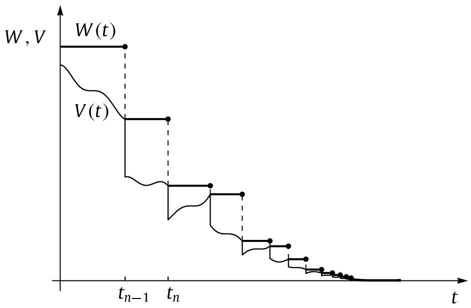

Fig. 3. The Lyapunov function V and the step function W for $\kappa < \kappa_{\mathrm{GUAS}}$.

we consider $t \in (t_{n-1}, t_n)$. It holds that $W(t) = V^-(t_{n-1})$ and $V(t) = V^-(t_{n-1}) + \int_{[t_{n-1},t)} \mathrm{d}V$ and therefore

$$W(t) - V(t) = -\left(V^+(t_{n-1}) - V^-(t_{n-1})\right) - \int_{t_{n-1}}^{t} \dot{V}\,\mathrm{d}t. \tag{65}$$

The last term in (65) can be bounded from above by the same conservative estimate as in (59):

$$\int_{t_{n-1}}^{t} \dot{V}\,\mathrm{d}t \le \frac{a_{\max} - a_{\min}}{2} \int_{t_{n-1}}^{t} |\gamma_N(t)|\mathrm{d}t \tag{66}$$

and we note that $\int_{t_{n-1}}^{t} |\gamma_N(t)|\mathrm{d}t \le \int_{t_{n-1}}^{t_n} |\gamma_N(t)|\mathrm{d}t$ for which we have the upper-bound (60). Hence, the difference between the step function W and the Lyapunov function V can, using the definition (62) of α, be bounded from below by

$$W(t) - V(t) \ge \frac{1}{2}(1-\alpha)\gamma_N^-(t_{n-1})^2, \tag{67}$$

which is non-negative under condition (39) meaning that the step function $W(t)$ is an upper-bound for $V(t)$.

All the conditions of Theorem 1 are therefore satisfied which proves that the equilibrium $\boldsymbol{x}^* = \mathbf{0}$ of the bouncing ball system is globally uniformly attractively stable under condition (39). □

Remark. If vibrations of the table are considered, then it naturally holds that $a_{\max} > 0$ and $a_{\min} < 0$. In that case, the above proof can be simplified by taking $\tilde{\mathrm{g}} = \mathrm{g}$ and using a slightly different estimate for the total variation of $g_N(t)$ over (t_{n-1}, t). For generality, this assumption has not been made in Theorem 1.

For the case of sinusoidal excitation $e(t) = -A\sin(\Omega t)$, it holds that $a_{\max} = -a_{\min} = A\Omega^2$. The condition (39) can be expressed in terms of the relative acceleration $\kappa = A\Omega^2/\mathrm{g}$ (16) as

$$\kappa < \frac{1-\bar{\varepsilon}^2}{1+\bar{\varepsilon}^2} =: \kappa_{\mathrm{GUAS}}. \tag{68}$$

This is a sufficient condition for globally uniform attractive stability of the equilibrium $\boldsymbol{x}^* = \mathbf{0}$. Fig. 3 depicts the time–history of the functions V and W for a sinusoidal excitation of the table. In contrast to the classical direct method of Lyapunov, where the Lyapunov function V is required to be non-increasing, the function V may decrease and increase on the interval (t_{n-1}, t_n), but cumulatively, it decreases on the time intervals between two consecutive impacts which is guaranteed by condition (68). The function V can therefore be regarded as a Lyapunov function in a generalized sense.

We might be tempted to think that the function W can be looked upon as a discrete-time Lyapunov function. A discrete-time Lyapunov function would be a (locally) positive definite function on the discrete state of the system at the impact time, which decreases under iterations of the impact map (see Section 6). Note, however, that the function W is constructed from the time evolution of V along solution curves and is therefore not a function of the discrete state. For this reason, it cannot be regarded as a discrete-time Lyapunov function, although it surely is related to a discrete-time Lyapunov function of the impact map. But there is a more fundamental difference: a discrete-time Lyapunov function only gives information on the state at discrete time-instants and does not check whether the solution converges to zero in between impacts. In contrast, the step function W is an upper-bound for V on the *whole* time domain.

Our considerations have so far ensured that the piecewise constant function

$$W(t) := V^-(t_{n-1}) \quad t \in (t_{n-1}, t_n] \tag{69}$$

is an upper-bound of the Lyapunov candidate function $V(t)$ which decreases and converges to zero. Subsequently, we will prove that W decreases to zero in a finite time under the conditions of Proposition 1, i.e. the attraction of the equilibrium is symptotic.

Proposition 2 (*Symptotic Attractive Stability*)**.** *If the conditions of Proposition 1 are met, then the equilibrium $\boldsymbol{x}^* = \mathbf{0}$ of the bouncing ball system (32) is globally symptotically attractive.*

Proof. The proposition uses the same conditions as Proposition 1 and we can therefore make use of the results of the proof of Proposition 1. Evaluation of (54) for $t = t_1$ with $g_N(t_1) = 0$ gives

$$0 \le g_N(t_0) + \gamma_N^+(t_0)\,(t_1 - t_0) - \frac{1}{2}\,(\mathrm{g} + a_{\min})\,(t_1 - t_0)^2, \tag{70}$$

which is an inequality of the form $0 \le f(t_1 - t_0)$ for the time lapse $t_1 - t_0 \ge 0$, where the right side of (70) is a concave quadratic function $f(t_1 - t_0)$ with a non-negative constant term $g_N(t_0)$. The function f is therefore non-negative between its two zeros, or, when only considering the positive domain, between the origin and the largest zero. We therefore obtain the upper-bound

$$t_1 - t_0 \le \frac{\gamma_N^+(t_0) + \sqrt{\gamma_N^+(t_0)^2 + 2(\mathrm{g} + a_{\min})g_N(t_0)}}{\mathrm{g} + a_{\min}} \tag{71}$$

of the time lapse between the initial time and the first (or next) collision. Similarly, evaluation of the inequality (54) for the non-impulsive time interval (t_{n-1}, t_n) with $g_N(t_{n-1}) = g_N(t_n) = 0$ gives

$$0 \le \gamma_N^+(t_{n-1})\,(t_n - t_{n-1}) - \frac{1}{2}\,(\mathrm{g} + a_{\min})\,(t_n - t_{n-1})^2, \tag{72}$$

where $\gamma_N^+(t_{n-1}) = -\varepsilon(t_{n-1})\gamma_N^-(t_{n-1})$, from which we obtain the upper-bound

$$t_n - t_{n-1} \le \frac{-2\varepsilon(t_{n-1})\gamma_N^-(t_{n-1})}{\mathrm{g} + a_{\min}} \le \frac{2\bar{\varepsilon}\sqrt{2W(t_n)}}{\mathrm{g} + a_{\min}} \tag{73}$$

of the time lapse between two consecutive collisions. The time-instant t_∞, for which the ball has come to rest on the table, can therefore be bounded from above by the sum

$$t_\infty - t_1 = \sum_{n=1}^{\infty}(t_{n+1} - t_n) \le \frac{2\sqrt{2}\bar{\varepsilon}}{\mathrm{g} + a_{\min}} \sum_{n=1}^{\infty} \sqrt{W(t_{n+1})}. \tag{74}$$

Recursive usage of the contraction property (64) gives the upper-bound

$$W(t_{n+1}) \le \alpha^n W(t_1) \quad \forall n \ge 1. \tag{75}$$

If (39) is fulfilled, then it holds that $0 \le \alpha < 1$ and the sum in (74) can be bounded from above by

$$t_\infty - t_1 \le \frac{2\sqrt{2}\bar{\varepsilon}}{\mathrm{g} + a_{\min}} \sum_{n=1}^{\infty} \sqrt{W(t_{n+1})} \le \frac{2\sqrt{2}\bar{\varepsilon}}{\mathrm{g} + a_{\min}} \sqrt{W(t_1)} \sum_{n=1}^{\infty} \sqrt{\alpha^n} = \frac{2\sqrt{2}\bar{\varepsilon}}{\mathrm{g} + a_{\min}} \sqrt{W(t_1)} \frac{\alpha^{\frac{1}{2}}}{1-\alpha^{\frac{1}{2}}} \quad (76)$$

in which we used the geometric series

$$\sum_{j=0}^{\infty} x^{\frac{1}{2}j} = \frac{1}{1-x^{\frac{1}{2}}}, \qquad \sum_{j=1}^{\infty} x^{\frac{1}{2}j} = \frac{x^{\frac{1}{2}}}{1-x^{\frac{1}{2}}} \quad 0 \le x < 1. \quad (77)$$

The time lapse between the initial time t_0 and the accumulation point t_∞ is therefore bounded from above by

$$t_\infty - t_0 \le \frac{\gamma_N^+(t_0) + \sqrt{\gamma_N^+(t_0)^2 + 2(\mathrm{g}+a_{\min})g_N(t_0)}}{\mathrm{g}+a_{\min}} + \frac{2\sqrt{2}\bar{\varepsilon}}{\mathrm{g} + a_{\min}} \sqrt{W(t_1)} \frac{\alpha^{\frac{1}{2}}}{1-\alpha^{\frac{1}{2}}} \quad (78)$$

with $W(t_1)$ bounded by (56) and $|\gamma_N^+(t_0)| \le |\gamma_N^-(t_0)|$. Hence, for any bounded initial condition $\boldsymbol{x}_0$, the solution $\boldsymbol{\varphi}(t, t_0, \boldsymbol{x}_0)$ converges in a finite time $t_\infty - t_0$ to the equilibrium $\boldsymbol{x}^* = \mathbf{0}$. □

Propositions 1 and 2 consider the same system with identical assumptions. We can therefore summarize the result:

Corollary 1. *Let the bouncing ball system (32) satisfy the bounds (13) of $e(t)$ and (11) on $\varepsilon(t)$. If it holds that*

$$\frac{\mathrm{g} + a_{\max}}{\mathrm{g} + a_{\min}} \bar{\varepsilon}^2 < 1,$$

then the equilibrium $\boldsymbol{x}^* = \mathbf{0}$ of the bouncing ball system is globally uniformly symptotically attractively stable.

Proof. The proof follows immediately from Propositions 1 and 2. □

Numerical simulations, which illustrate the above theoretical results, are shown in Fig. 4 for $t_0 = 0$, $g_N(t_0) = 0$, $\gamma_N^+(t_0) = 8$, $\varepsilon = 0.8$ and $\kappa = 0.2 < \kappa_{\mathrm{GUAS}}$. The trajectory of the bouncing ball, Fig. 4(a), shows that the solution is attracted to the equilibrium in finite time through an infinite number of impacts. The corresponding state space is shown in Fig. 4(b). The Lyapunov function V evaluated along the solution curve, depicted in Fig. 4(c), is oscillating but is bounded from above by the decreasing step function $W(t)$ as depicted in Fig. 3.

6. Periodic solutions

A sufficient condition (39) for global uniform symptotic stability of the equilibrium of the bouncing ball system has been derived in the previous sections. In this section, we would like to shed some light on the conservativeness of the condition (39) by looking at the existence of periodic motion of the bouncing ball system. The co-existence of periodic motion and the equilibrium indicates that the equilibrium is at most locally attractive.

Periodic motion of the bouncing ball system can conveniently be studied with a discrete map (see for instance [31,33]), referred to as the impact map, which describes the motion of the bouncing ball only in discrete time, that is to say at collision time-instants $\{t_n\}$ when the ball hits the table subjected to the kinematic excitation $e(t)$. The post-impact relative velocity $\gamma_N^+(t_n)$ is sampled together with the collision time t_n at each impact of the ball with the table and related to the variables t_{n+1} and $\gamma_N^+(t_{n+1})$ of the next impact. The trajectory of the bouncing ball is therefore described by a sequence of impact events, characterized by the aforementioned coordinates t_n and $\gamma_N^+(t_n)$. The impact map is first derived for an arbitrary excitation $e(t)$ of the table and a time-varying restitution coefficient $\varepsilon(t)$. For the subsequent analysis, $e(t)$ is chosen as $e(t) = -A\sin(\Omega t)$ and the restitution coefficient is assumed to be constant. The map is transcendental in the case of a harmonic excitation and has an implicit structure.

Between two consecutive impacts, say on the open time interval (t_n, t_{n+1}), the ball is moving only under the action of gravity and it holds that $\dot{g}_N(t) = \gamma_N(t)$ and $\dot{\gamma}_N(t) = -\mathrm{g} - \ddot{e}(t)$. Integration of the differential equations over the non-impulsive time interval (t_n, t_{n+1}) gives

$$g_N(t_{n+1}) = g_N(t_n) + \left(\gamma_N^+(t_n) + \dot{e}(t_n)\right)(t_{n+1}-t_n) - \frac{1}{2}\mathrm{g}(t_{n+1}-t_n)^2 - e(t_{n+1}) + e(t_n), \quad (79)$$

$$\gamma_N^-(t_{n+1}) = \gamma_N^+(t_n) - \mathrm{g}(t_{n+1}-t_n) - \dot{e}(t_{n+1}) + \dot{e}(t_n). \quad (80)$$

The contact distance vanishes at collision times, i.e. $g_N(t_n) = g_N(t_{n+1}) = 0$, and (79) becomes

$$0 = -\frac{1}{2}\mathrm{g}\,(t_{n+1}-t_n)^2 + \left(\gamma_N^+(t_n) + \dot{e}(t_n)\right)(t_{n+1}-t_n) - e(t_{n+1}) + e(t_n), \quad (81)$$

which is an implicit equation for t_{n+1}. Using the impact law (10), $\gamma_N^+(t_{n+1}) = -\varepsilon(t_{n+1})\gamma_N^-(t_{n+1})$, together with (80) yields an expression for $\gamma_N^+(t_{n+1})$:

$$0 = -\gamma_N^+(t_{n+1}) - \varepsilon(t_{n+1})\gamma_N^+(t_n) + \varepsilon(t_{n+1})\mathrm{g}(t_{n+1}-t_n) + \varepsilon(t_{n+1})\left(\dot{e}(t_{n+1}) - \dot{e}(t_n)\right). \quad (82)$$

The two equations (81) and (82) form an implicit map $\left(t_n, \gamma_N^+(t_n)\right) \mapsto \left(t_{n+1}, \gamma_N^+(t_{n+1})\right)$.

In the following, $e(t)$ is chosen as $e(t) = -A\sin(\Omega t)$ and the restitution coefficient ε is assumed to be constant. Furthermore, in order to reduce the parameter space, the equations (81) and (82) are rewritten in dimensionless form, defining

$$\tau_n := \frac{\Omega}{2\pi} t_n, \qquad w_n := \frac{\Omega}{\pi \mathrm{g}} \gamma_N^+(t_n), \quad (83)$$

where τ_n is the dimensionless time and w_n is the dimensionless post-impact contact velocity. Substitution of (83) into the equations (81) and (82) and using the relative acceleration κ (16), we obtain the implicit map

$$\boldsymbol{G}(\boldsymbol{z}_n, \boldsymbol{z}_{n+1}) = \begin{bmatrix} G_1(\boldsymbol{z}_n, \boldsymbol{z}_{n+1}) \\ G_2(\boldsymbol{z}_n, \boldsymbol{z}_{n+1}) \end{bmatrix} = \mathbf{0}, \quad n \in \mathbb{Z}_0, \quad (84)$$

where $\boldsymbol{z}_n = \begin{bmatrix}\tau_n & w_n\end{bmatrix}^{\mathrm{T}}$ with

$$G_1 = \frac{\kappa}{2\pi^2}\left(\sin(2\pi\tau_{n+1}) - \sin(2\pi\tau_n)\right) + \left(w_n - \frac{\kappa}{\pi}\cos(2\pi\tau_n)\right)(\tau_{n+1}-\tau_n) - (\tau_{n+1}-\tau_n)^2,$$

$$G_2 = -w_{n+1} - \varepsilon\, w_n + 2\varepsilon(\tau_{n+1}-\tau_n) - \varepsilon\frac{\kappa}{\pi}\left(\cos(2\pi\tau_{n+1}) - \cos(2\pi\tau_n)\right).$$

The parameter space for the dimensionless map (84) has reduced from the four parameters A, Ω, ε and g to two parameters, being the relative acceleration of the table κ and the coefficient of restitution ε.

Fixed points $\boldsymbol{z}^*$ of the impact map (84) fulfil $\boldsymbol{G}(\boldsymbol{z}^*, \boldsymbol{z}^*) = \mathbf{0}$ which results in

$$G_1(\boldsymbol{z}^*, \boldsymbol{z}^*) : 0 = 0, \qquad G_2(\boldsymbol{z}^*, \boldsymbol{z}^*) : -w^* - \varepsilon\, w^* = 0, \quad (85)$$

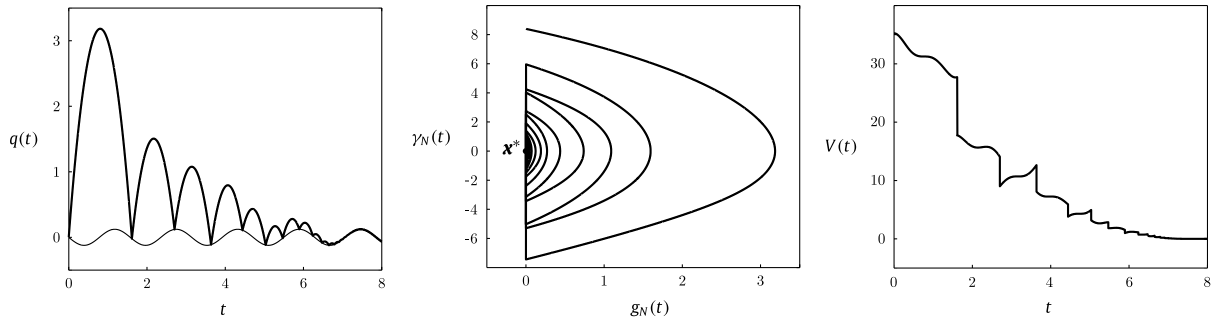

(a) (b) (c)

Fig. 4. Numerical simulation of the bouncing ball system.

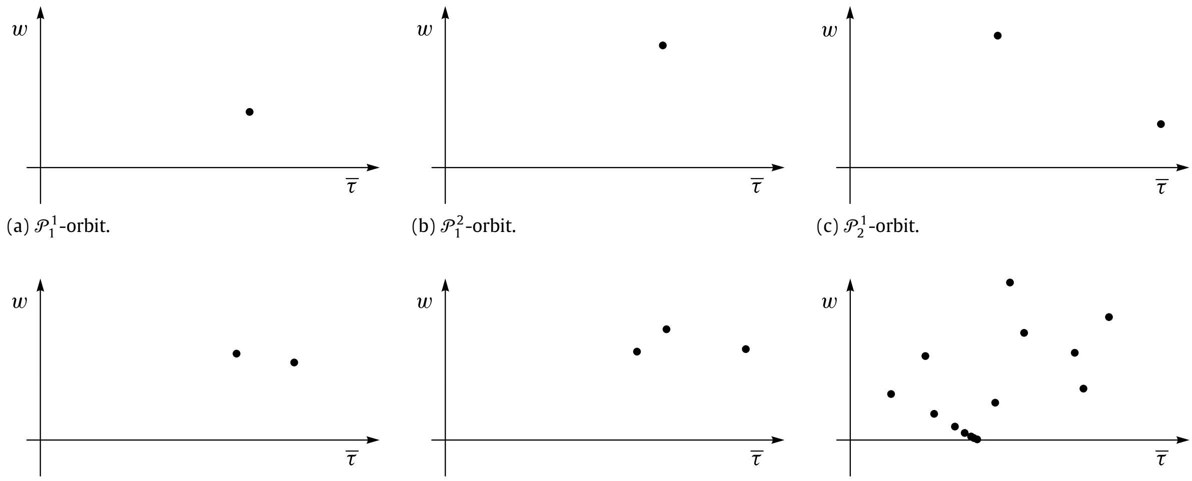

(a) $\mathcal{P}_1^1$-orbit. (b) $\mathcal{P}_1^2$-orbit. (c) $\mathcal{P}_2^1$-orbit.

(d) $\mathcal{P}_2^2$-orbit. (e) $\mathcal{P}_3^3$-orbit. (f) $\mathcal{P}_\infty^7$-orbit.

Fig. 5. Discrete-time representation of $\mathcal{P}_l^k$-orbits.

and it therefore holds that

$$\boldsymbol{z}^* = \begin{bmatrix} \tau^* \\ w^* \end{bmatrix} = \begin{bmatrix} \tau^* \\ 0 \end{bmatrix}. \tag{86}$$

The fixed points of the impact map therefore correspond to $g_N(t^*) = 0$ and $\gamma_N^+(t^*) = 0$, with $t^* = 2\pi/\Omega\tau^*$, i.e. to the case where the ball is in persistent contact with the table. It is not surprising that a state of persistent contact is a fixed point of the map since the impact law (10) holds for all time-instants for which $g_N(t) = 0$, i.e. also when $\gamma_N^-(t) = \gamma_N^+(t) = 0$. The impact map is able to describe how the ball comes into persistent contact through an accumulation of impacts. Such a right-accumulation point involves infinitely many impacts of the ball with the table within a finite time, corresponding to infinitely many iterations of the impact map. The impact map is therefore not able to describe the following non-impulsive motion of the ball, because (84) assumes free flight between consecutive impacts. If $\kappa \leq 1$, then the fixed points of the impact map correspond to the equilibrium position of the bouncing ball system (32). If $\kappa > 1$, then the equilibrium does not exist and persistent contact will be lost when the acceleration of the downwards moving table exceeds the gravitational acceleration g.

The bouncing ball system exhibits a plethora of periodic motions. Periodic motions which do not contain phases of persistent contact can conveniently be described and be characterized by the impact map (84).

Definition 4. An orbit of the impact map $\boldsymbol{G}$ (84) in the (τ, w)-space is called an l-periodic orbit of order k, denoted as $\mathcal{P}_l^k$-orbit, if it holds that

$$\begin{bmatrix} \tau_{n+l} \\ w_{n+l} \end{bmatrix} = \begin{bmatrix} \tau_n \\ w_n \end{bmatrix} + \begin{bmatrix} k \\ 0 \end{bmatrix}, \quad l, k \geq 1, \forall n \in \mathbb{Z}_0. \tag{87}$$

The period time of a $\mathcal{P}_l^k$-orbit is $\frac{2\pi}{\Omega}k$ and l impacts occur within one period. A $\mathcal{P}_l^k$-orbit is therefore k-periodic with respect to the excitation frequency Ω and l-periodic with respect to the impact map (84). Figs. 5 and 6 give an overview on some specific $\mathcal{P}_l^k$-orbits in the (τ, w)-space and in continuous-time representation. In order to depict these trajectories as l-periodic fixed points in the (τ, w)-space, the dimensionless time axis is folded using $\bar{\tau} = \tau \bmod 1$. Figs. 5(a) and 6(a) depict 1-periodic orbits of order 1 and Figs. 5(b) and 6(b) of order 2, respectively. This case will be investigated more precisely in the subsequent analysis. Figs. 5(c) and 6(c) show a $\mathcal{P}_2^1$-orbit, whereas Figs. 5(d) and 6(d) show a $\mathcal{P}_2^2$-orbit. Figs. 5(e) and 6(e) illustrate a $\mathcal{P}_3^3$-orbit. The $\mathcal{P}_\infty^7$-orbit, shown in Figs. 5(f) and 6(f), contains a right-accumulation point and a phase of persistent contact within each period. Such periodic motions cannot be described by the impact map (84) and have to be found by numerical integration of the measure differential inclusion (32). Note that the right-accumulation point (or 'Zeno' point), which is present in the $\mathcal{P}_\infty^7$-orbit, is not an equilibrium point.

We first consider $\mathcal{P}_1^k$-orbits, i.e. 1-periodic orbits with arbitrary order k. For a $\mathcal{P}_1^k$-orbit we define

$$\tau^{k,1} = \tau_n \bmod 1, \qquad w^{k,1} = w_n \quad \forall n. \tag{88}$$

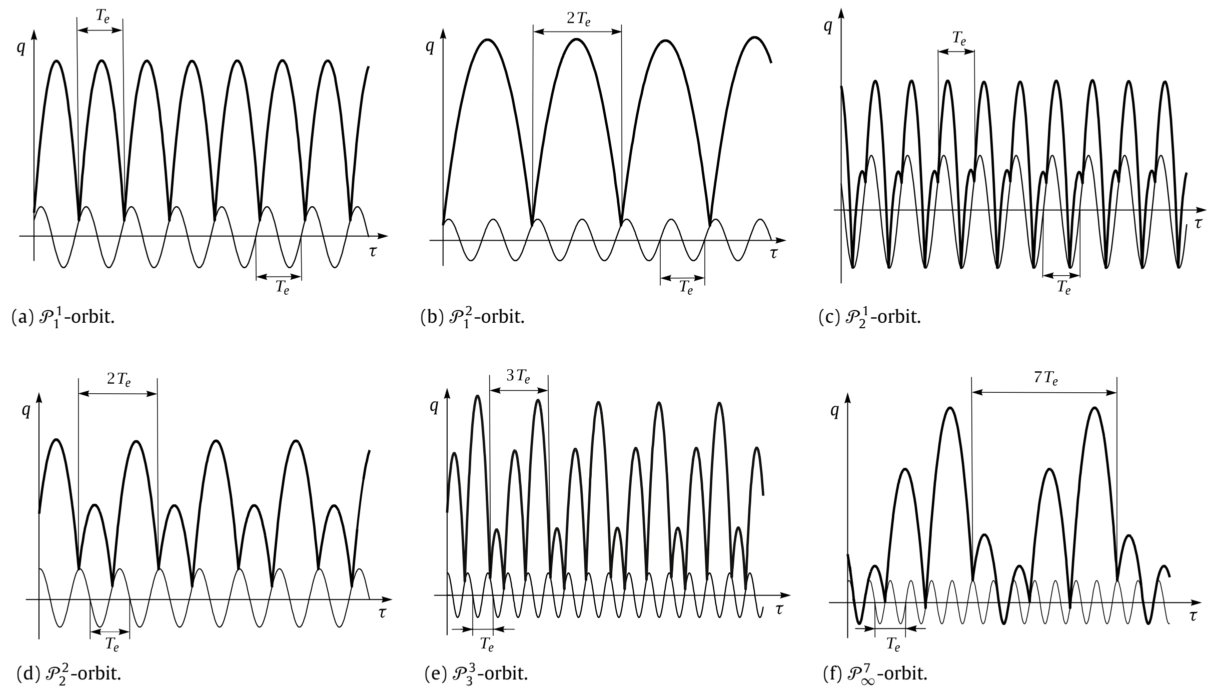

Fig. 6. Continuous-time representation of $\mathcal{P}_l^k$-orbits.

Substitution of (87) with $l = 1$ into the impact map (84) yields:

$$G_1 = \left(w^{k,1} - \frac{\kappa}{\pi}\cos(2\pi\tau^{k,1})\right)k - k^2 = 0, \qquad G_2 = -w^{k,1} - \varepsilon\, w^{k,1} + 2\varepsilon k = 0. \tag{89}$$

Eq. (89) can be solved for $w^{k,1}$ and $\tau^{k,1}$, which results in

$$w^{k,1} = \frac{2\varepsilon}{1+\varepsilon}k \tag{90}$$

and

$$\cos(2\pi\tau^{k,1}) = -\frac{1-\varepsilon}{1+\varepsilon}\frac{\pi k}{\kappa}. \tag{91}$$

Hence, $\mathcal{P}_1^k$-orbits exist if and only if

$$\left|-\frac{1-\varepsilon}{1+\varepsilon}\frac{\pi k}{\kappa}\right| \le 1 \quad \Leftrightarrow \quad \kappa \ge \frac{1-\varepsilon}{1+\varepsilon}\pi k =: \kappa_1^k. \tag{92}$$

Eq. (92) has one solution $\tau^{k,1} = \frac{1}{2}$ if $\kappa = \kappa_1^k$ and two distinct solutions symmetric around $\frac{1}{2}$ if $\kappa > \kappa_1^k$. The stability of the $\mathcal{P}_1^k$-orbits can be obtained from the linearized impact map [31,46]

$$\mathbf{0} = \frac{\partial \boldsymbol{G}}{\partial \boldsymbol{z}_n}\boldsymbol{y}_n + \frac{\partial \boldsymbol{G}}{\partial \boldsymbol{z}_{n+1}}\boldsymbol{y}_{n+1}, \tag{93}$$

where $\boldsymbol{y}_n$ are the perturbations of $\boldsymbol{z}_n$ with respect to the $\mathcal{P}_1^k$-orbit and

$$\frac{\partial \boldsymbol{G}}{\partial \boldsymbol{z}_n} = \begin{bmatrix} 2k\kappa\sigma + \dfrac{2k}{1+\varepsilon} & k \\ -2\varepsilon(1+\kappa\sigma) & -\varepsilon \end{bmatrix}, \qquad \frac{\partial \boldsymbol{G}}{\partial \boldsymbol{z}_{n+1}} = \begin{bmatrix} -\dfrac{2k}{1+\varepsilon} & 0 \\ 2\varepsilon(1+\kappa\sigma) & -1 \end{bmatrix}, \tag{94}$$

with the abbreviation

$$\sigma := \sin(2\pi\tau^{k,1}), \tag{95}$$

are the partial derivatives of the impact map evaluated at the $\mathcal{P}_1^k$-orbit (88). The propagation of the perturbation is therefore described by the linear map

$$\boldsymbol{y}_{n+1} = \boldsymbol{A}\boldsymbol{y}_n, \tag{96}$$

where

$$\boldsymbol{A} = -\left(\frac{\partial \boldsymbol{G}}{\partial \boldsymbol{z}_{n+1}}\right)^{-1}\frac{\partial \boldsymbol{G}}{\partial \boldsymbol{z}_n} = \begin{bmatrix} 1+(1+\varepsilon)\kappa\sigma & \dfrac{1+\varepsilon}{2} \\ 2\varepsilon(1+\varepsilon)\kappa\sigma(1+\kappa\sigma) & \varepsilon(1+\varepsilon)\kappa\sigma+\varepsilon^2 \end{bmatrix} \tag{97}$$

is the linearization matrix. The matrix $\boldsymbol{A}$ has the characteristic polynomial $\lambda^2 + \alpha_1\lambda + \alpha_2 = 0$ with the coefficients

$$\alpha_1 = -\operatorname{trace}(\boldsymbol{A}) = -1 - \varepsilon^2 - (1+\varepsilon)^2\kappa\sigma, \qquad \alpha_2 = \det(\boldsymbol{A}) = \varepsilon^2. \tag{98}$$

The linear map is asymptotically stable if the matrix $\boldsymbol{A}$ has eigenvalues with a magnitude smaller than unity, i.e. if the Schur–Cohn conditions [47] are fulfilled:

$$1 \pm \alpha_1 + \alpha_2 > 0, \qquad 1 \pm \alpha_2 > 0. \tag{99}$$

The condition $1 \pm \alpha_2 > 0$ is naturally fulfilled for $0 \le \varepsilon < 1$. The condition $1 + \alpha_1 + \alpha_2 > 0$ yields

$$-(1+\varepsilon)^2\kappa\sigma > 0 \quad \Leftrightarrow \quad \sigma < 0, \tag{100}$$

which implies the stability condition $\tau^{k,1} > \frac{1}{2}$, i.e. $\mathcal{P}_1^k$-orbits associated to the value of $\tau^{k,1} < \frac{1}{2}$ are unstable. The condition $1 - \alpha_1 + \alpha_2 > 0$ yields

$$2 + 2\varepsilon^2 + (1+\varepsilon)^2\kappa\sigma > 0, \tag{101}$$

which gives together with $\sigma^2 = 1 - \left(\kappa_1^k\right)^2$, see (91), (92) and (95), and $\sigma < 0$ (100) the stability condition

$$\kappa^2 < \left(\kappa_1^k\right)^2 + \frac{4(1+\varepsilon^2)^2}{(1+\varepsilon)^4}. \tag{102}$$

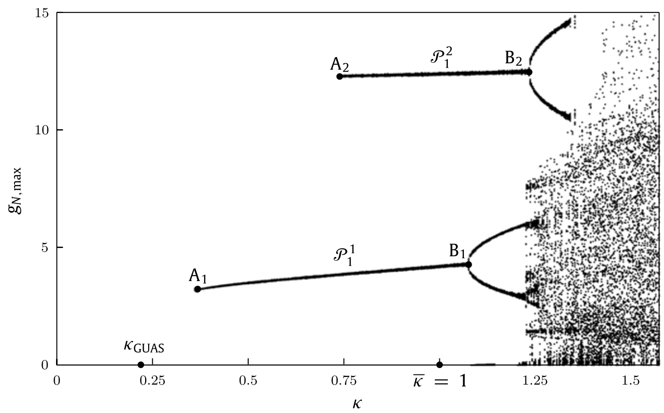

Fig. 7. Bifurcation diagram for $\varepsilon = 0.8$.

We therefore conclude that $\mathcal{P}_1^k$-orbits associated with $\tau^{k,1} > \frac{1}{2}$ are locally attractively stable if

$$\kappa_1^k := \frac{1-\varepsilon}{1+\varepsilon}\pi k < \kappa < \sqrt{\frac{4(1+\varepsilon^2)^2}{(1+\varepsilon)^4} + \left(\kappa_1^k\right)^2} =: \kappa_{-1}^k. \qquad (103)$$

For $\kappa = \kappa_1^k$, the linearization has a maximal eigenvalue $\lambda_{\max} = 1$ and for $\kappa = \kappa_{-1}^k$ the maximal eigenvalue $\lambda_{\max} = -1$, where $\lambda_{\max}$ is the eigenvalue with the largest spectral radius. Using standard results from bifurcation theory, we infer that fold bifurcations occur for $\kappa = \kappa_1^k$ and period-doubling (or flip) bifurcations for $\kappa = \kappa_{-1}^k$, where $k \geq 1$.

A bifurcation diagram for the bouncing ball system has been constructed using the so-called "brute force" technique [48], a simple numerical method which shows only attracting limit sets. Starting from a chosen initial condition and a chosen value of κ, the system (32) is simulated over 300 periods of the excitation frequency Ω. For each time interval $[t_n, t_{n+1}]$, between two consecutive impacts, the maximal contact distance

$$g_{N,\max} = \max_{t\in[t_n,t_{n+1}]} g_N(t) \qquad (104)$$

can be computed. The last 50 values of the maximal contact distance $g_{N,\max}$ are plotted as points in the bifurcation diagram. Subsequently, the value of κ is increased with 0.001 and the last state of the previous simulation is used as new initial condition. In this way, the solution for each κ is allowed to approach an attractor before the 50 points are plotted. If the solution is attracted to a $\mathcal{P}_1^k$-orbit, then the 50 points will be approximately located on top of each other, while l heaps of points can be observed for a $\mathcal{P}_l^k$-attractor. Chaotic attractors appear as clouds of points in the brute force bifurcation diagram. The bifurcation diagram for $\varepsilon = 0.8$ is shown in Fig. 7 where the associated branches of $\mathcal{P}_1^1$-orbits and $\mathcal{P}_1^2$-orbits are shown. The equilibrium branch is located on the axis $g_{N,\max} = 0$ for $\kappa \leq \bar{\kappa} = 1$. As has been shown previously, $\mathcal{P}_1^k$-orbits are created at fold bifurcations A_k for $\kappa = \kappa_1^k$. Note that the brute force technique only reveals attractively stable limit sets. Therefore, the unstable branches of the $\mathcal{P}_1^k$-orbits are not depicted here. The branches of attractively stable $\mathcal{P}_1^k$-orbits undergo period-doubling bifurcations at the bifurcation points B_k for $\kappa = \kappa_{-1}^k$. Two branches belonging to the same $\mathcal{P}_2^{2k}$ emerge at the bifurcation points B_k. An example of a $\mathcal{P}_2^2$-orbit is shown in Fig. 6(d). The two different maximal heights of the periodic orbit appear as two separate branches in the bifurcation diagram.

When looking at Fig. 7 one is tempted to think that no periodic motion and chaotic attractors exist for $\kappa < \kappa_1^1$ and that the equilibrium is globally attractive for $\kappa < \kappa_1^1$. At this point, we have to note that the numerically generated bifurcation diagram is not complete. The bifurcation diagram 7 already shows various kinds of periodic motion as well as chaotic attractors, but many other periodic motions may co-exist with the shown attractors, e.g. branches exist of $\mathcal{P}_l^k$-orbits with $l > k$ (such a case is depicted in Fig. 6(c) for a $\mathcal{P}_2^1$-orbit). How can we be sure that no co-existent attractors exist for $\kappa < \kappa_1^1$? The use of Proposition 1 now becomes apparent. We are not able to consider the plethora of periodic motions and aperiodic limit sets, but Proposition 1 rigorously proves that the equilibrium is *globally* symptotically attractively stable if condition (68) holds, i.e. $\kappa < \kappa_{GUAS}$. Proposition 1 gives a *sufficient* condition, in other words the upper-bound κ_{GUAS} is a conservative estimate. The bifurcation diagram 7 gives us some idea about how conservative κ_{GUAS} is.

7. Conclusions

In this paper, a Lyapunov-like theorem (Theorem 1) to prove the conditional global uniform attractive stability of the equilibria of non-autonomous MDIs has been presented, which can be regarded as an extension of Lyapunov's direct method to (generalized) Lyapunov functions which may also temporarily increase along solution curves. The conditions of Theorem 1 look more complicated than those of the standard Lyapunov's direct method, because a decreasing step function $W(t)$ above the Lyapunov function $V(t)$ (evaluated along solution curves) has to be found. The key point in Theorem 1 is, that the conditions on the Lyapunov function are weaker: the Lyapunov function is allowed to oscillate and may temporarily increase along solution curves. Theorem 1 therefore gives more freedom to choose the Lyapunov function, thereby allowing the choice of Lyapunov functions with a clear physical meaning.

A sufficient condition for the global uniform symptotic attractive stability of the equilibrium of the bouncing ball system with an arbitrary motion of the table and time-varying restitution coefficient has been proved by using Theorem 1. As Lyapunov function we were able to choose a relatively simple function, being the sum of a quadratic term and a linear term, which for harmonic excitation agrees with the total mechanical energy (40) of the equivalent forced system (Fig. 1(b)). Furthermore, it has been proved that the attractivity of the equilibrium of the bouncing ball system is symptotic.

A possible application of the stability results of the bouncing ball system can be sought in tracking and position control problems of robotic manipulators with unilateral constraints [49]. For instance, one can consider a robotic task in which the end-effector has to place an object on a moving support, or, equivalently, on a stationary support but under the influence of an uncertain forcing. If the closed loop dynamics of the end-effector is equivalent to that of the bouncing ball system, then Proposition 1 assures the finite-time stabilization of the object on the support. Proposition 1 might therefore open new directions for feed-back control design of mechanical systems with unilateral constraints.

References

[1] Ch. Glocker, Set-Valued Force Laws, Dynamics of Non-Smooth Systems, in: Lecture Notes in Applied Mechanics, vol. 1, Springer-Verlag, Berlin, 2001.

[2] R.I. Leine, H. Nijmeijer, Dynamics and Bifurcations of Non-Smooth Mechanical Systems, in: Lecture Notes in Applied and Computational Mechanics, vol. 18, Springer Verlag, Berlin, 2004.

[3] A. Fidlin, On the asymptotic analysis of discontinuous systems, Zeitschrift für angewandte Mathematik und Mechanik 82 (2) (2002) 75–88.

[4] B. Brogliato, Nonsmooth Mechanics. Models, Dynamics and Control, 2nd ed., in: Communications and Control Engineering, Springer, London, 1999.

[5] A.J. van der Schaft, J.M. Schumacher, An Introduction to Hybrid Dynamical Systems, in: Lecture Notes in Control and Information Sciences, vol. 251, Springer, London, 2000.

[6] R. Goebel, A.R. Teel, Solutions to hybrid inclusions via set and graphical convergence with stability theory applications, Automatica 42 (2006) 573–587.
[7] J. Lygeros, K. Johansson, S. Simić, J. Zhang, S. Sastry, Dynamical properties of hybrid automata, IEEE Transactions on Automatic Control 48 (1) (2003) 2–17.
[8] Y. Or, A.D. Ames, Stability of Zeno equilibria in Lagrangian hybrid systems, in: Proceedings of the IEEE Conference on Decision and Control, 2008, pp. 2770–2775.
[9] A.D. Ames, H. Zheng, R.D. Gregg, S. Sastry, Is there life after Zeno? Taking executions past the breaking (Zeno) point, in: Proceedings of the American Control Conference, 2006, pp. 2652–2657.
[10] M. Heymann, F. Lin, G. Meyer, S. Resmerita, Analysis of Zeno behaviors in a class of hybrid systems, IEEE Transactions on Automatic Control 50 (3) (2005) 376–384.
[11] A.B. Nordmark, P.T. Piiroinen, Simulation and stability analysis of impacting systems with complete chattering, International Journal of Nonlinear Dynamics and Chaos in Engineering Systems 58 (1) (2009) 85–106.
[12] A.F. Filippov, Differential Equations with Discontinuous Right-hand Sides, Kluwer Academic, Dordrecht, 1988.
[13] M. Monteiro Marques, Differential Inclusions in Nonsmooth Mechanical Systems, Birkhäuser, Basel, 1993.
[14] J.J. Moreau, Unilateral contact and dry friction in finite freedom dynamics, in: J.J. Moreau, P.D. Panagiotopoulos (Eds.), Non-Smooth Mechanics and Applications, in: CISM Courses and Lectures, vol. 302, Springer, Wien, 1988, pp. 1–82.
[15] R.I. Leine, N. van de Wouw, Stability and Convergence of Mechanical Systems with Unilateral Constraints, in: Lecture Notes in Applied and Computational Mechanics, vol. 36, Springer Verlag, Berlin, 2008.
[16] Ch. Glocker, Models of non-smooth switches in electrical systems, International Journal of Circuit Theory and Applications 33 (3) (2005) 205–234.
[17] R.I. Leine, D.H. van Campen, Bifurcation phenomena in non-smooth dynamical systems, European Journal of Mechanics – A/Solids 25 (2006) 595–616.
[18] R.I. Leine, Bifurcations of equilibria in non-smooth continuous systems, Physica D 223 (2006) 121–137.
[19] B. Brogliato, Absolute stability and the Lagrange–Dirichlet theorem with monotone multivalued mappings, Systems & Control Letters 51 (2004) 343–353.
[20] A. Rantzer, M. Johansson, Piecewise linear quadratic optimal control, IEEE Transactions on Automatic Control 45 (4) (2000) 629–637.
[21] M. Arcak, P. Kokotović, Observer-based control of systems with slope-restricted nonlinearities, IEEE Transactions on Automatic Control 46 (2001) 1–5.
[22] N.J. Mallon, N. van de Wouw, D. Putra, H. Nijmeijer, Friction compensation in a controlled one-link robot using a reduced-order observer, IEEE Transactions on Control Systems Technology 14 (2) (2006) 374–383.
[23] S. Galeani, L. Menini, A. Tornambè, A parameterization of exponentially stabilizing controllers for linear mechanical systems subject to non-smooth impacts, IFAC Annual Reviews in Control 28 (1) (2004) 13–21.
[24] M. Indri, A. Tornambè, Control of a series of carts in the case of nonsmooth unilateral impacts, Applied Mathematics Letters 19 (6) (2006) 541–546.
[25] L. Menini, A. Tornambè, Exponential and BIBS stabilisation of one degree of freedom mechanical systems subject to single non-smooth impacts, IEE Proceedings - Control Theory and Applications 148 (2) (2001) 147–155.
[26] N. van de Wouw, R.I. Leine, Attractivity of equilibrium sets of systems with dry friction, International Journal of Nonlinear Dynamics and Chaos in Engineering Systems 35 (1) (2004) 19–39.
[27] R.I. Leine, N. van de Wouw, Stability properties of equilibrium sets of nonlinear mechanical systems with dry friction and impact, International Journal of Nonlinear Dynamics and Chaos in Engineering Systems 51 (4) (2008) 551–583.
[28] R.I. Leine, N. van de Wouw, Uniform convergence of monotone measure differential inclusions: with application to the control of mechanical systems with unilateral constraints, International Journal of Bifurcation and Chaos 15 (5) (2008) 1435–1457.
[29] N. van de Wouw, R.I. Leine, H. Nijmeijer, Controlling attractivity of friction-induced equilibrium sets, in: Proceedings of the 44th IEEE Conference on Decision and Control and European Control Conference ECC, IEEE, Sevilla, 2005, pp. 2610–2615.
[30] N. van de Wouw, R.I. Leine, Stability of stationary sets in nonlinear systems with set-valued friction, in: Proceedings of the 45th IEEE Conference on Decision and Control and European Control Conference ECC, IEEE, San Diego.
[31] J.M. Luck, A. Mehta, Bouncing ball with a finite restitution: chattering, locking, and chaos, Physical Review E 48 (5) (1993) 3988–3997.
[32] R.M. Everson, Chaotic dynamics of a bouncing ball, Physica D 19 (3) (1986) 355–383.
[33] S. Giusepponi, F. Marchesoni, The chattering dynamics of an ideal bouncing ball, Europhysics Letters 64 (2003) 36–42.
[34] J. Guckenheimer, P. Holmes, Nonlinear Oscillations, Dynamical Systems, and Bifurcations of Vector Fields, in: Applied Mathematical Sciences, vol. 42, Springer-Verlag, New York, 1983.
[35] N. Tuffilaro, T. Abbott, J. Reilly, An Experimental Approach to Nonlinear Dynamics and Chaos, Addison Wesley, New York, 1992.
[36] R. Klages, I.F. Barna, L. Mátyás, Spiral modes in the diffusion of a granular particle on a vibrating surface, Physics Letters A 333 (2002) 79–84.
[37] T. Heimsch, R.I. Leine, Lyapunov stability theory for non-smooth non-autonomous mechanical systems applied to the bouncing ball problem, in: Proceedings of the ASME 2009 International Design Engineering Technical Conferences & Computers and Information in Engineering Conference IDETC/CIE 2009, DETC/MSNDC-87185, San Diego, USA.
[38] Y. Or, A.R. Teel, Zeno stability of the set-valued bouncing ball, IEEE Transactions on Automatic Control 56 (2) (2011) 447–452.
[39] J.J. Moreau, Bounded variation in time, in: J.J. Moreau, P.D. Panagiotopoulos, G. Strang (Eds.), Topics in Nonsmooth Mechanics, Birkhäuser, Basel, Boston, Berlin, 1988, pp. 1–74.
[40] V. Acary, B. Brogliato, Numerical methods for nonsmooth dynamical systems, in: Applications in Mechanics and Electronics, in: Lecture Notes in Applied and Computational Mechanics, vol. 35, Springer, Berlin, 2008.
[41] M. Schatzman, Uniqueness and continuous dependence on data for one dimensional impact problems, Mathematical and Computational Modelling 28 (1998) 1–18.
[42] H. K. Khalil, Nonlinear Systems, Prentice-Hall, New Jersey, 1996.
[43] D. Angeli, B. Ingalls, E.D. Sontag, Y. Wang, Uniform global asymptotic stability of differential inclusions, Journal of Dynamical and Control Systems 10 (3) (2004) 391–412.
[44] R. Goebel, R.G. Sanfelice, A.R. Teel, Invariance principles for switching systems via hybrid systems techniques, Systems & Control Letters 57 (12) (2008) 980–986.
[45] R. Goebel, A.R. Teel, Lyapunov characterization of Zeno behavior in hybrid systems, in: Proceedings of the IEEE Conference on Decision and Control, 2008, 2752–2757.
[46] T. Heimsch, Lyapunov stability theory for nonsmooth non-autonomous mechanical systems applied to the bouncing ball problem, Master's Thesis, ETH Zurich under supervision of R.I. Leine, 2008.
[47] M. Marden, Geometry of polynomials, in: Mathematical Surveys and Monographs, vol. 3, American Mathematical Society, Providence, Rhode Island, 1989.
[48] T.S. Parker, L.O. Chua, Practical Numerical Algorithms for Chaotic Systems, Springer-Verlag, New York, 1989.
[49] C. Morărescu, B. Brogliato, Passivity-based switching control of flexible-joint complementarity mechanical systems, Automatica 46 (1) (2010) 160–166.